Naval Research Laboratory
Washington, DC 20375-5320

NRL/5310/MR—2021/10

Design of a Cylindrical Array for Multifunction Use

ANNA STUMME

MARK DORSEY

JOHN A. VALENZI

Radar Analysis Branch
Radar Division

October 5, 2021

REPORT DOCUMENTATION PAGE

Form Approved
OMB No. 0704-0188

1. REPORT DATE *(DD-MM-YYYY)*
05-10-2021

2. REPORT TYPE
NRL Memorandum Report

3. DATES COVERED *(From - To)*
2018 – 2021

4. TITLE AND SUBTITLE
Design of a Cylindrical Array for Multifunction Use

5a. CONTRACT NUMBER

5b. GRANT NUMBER

5c. PROGRAM ELEMENT NUMBER
62271N

6. AUTHOR(S)
Anna M. Stumme, Mark W. Dorsey, and John A. Valenzi

5d. PROJECT NUMBER

5e. TASK NUMBER
EW-271-001

5f. WORK UNIT NUMBER
6B10

7. PERFORMING ORGANIZATION NAME(S) AND ADDRESS(ES)
Naval Research Laboratory
4555 Overlook Avenue, SW
Washington, DC 20375-5320

8. PERFORMING ORGANIZATION REPORT NUMBER
NRL/5310/MR--2021/10

9. SPONSORING / MONITORING AGENCY NAME(S) AND ADDRESS(ES)
Naval Research Laboratory
4555 Overlook Avenue, SW
Washington, DC 20375-532

10. SPONSOR / MONITOR'S ACRONYM(S)
NRL Base Program

11. SPONSOR / MONITOR'S REPORT NUMBER(S)

12. DISTRIBUTION / AVAILABILITY STATEMENT
DISTRIBUTION STATEMENT A: Approved for public release; distribution is unlimited.

13. SUPPLEMENTARY NOTES

14. ABSTRACT

In recent years, the Navy has looked to transition to multifunction array apertures to reduce the size of ”antenna farms” on ships' masts and other space constrained areas. Cylindrical phased arrays are an attractive aperture for multifunction radio frequency (RF) systems requiring a 360-deg field of view because of their immense flexibility in radiation pattern performance. Cylindrical arrays offer the pattern versatility to operate with multiple pattern shapes. In one mode, cylindrical arrays form directional patterns that are scanned throughout the azimuth plane with nearly constant gain, beamwidth, sidelobe level, and polarization properties – avoiding the degradation faced by multi-faced planar array systems. Apertures must support a wide operational bandwidth to support wide ranging functions. This report presents the design of an all metal cylindrical array of stepped-notch elements, which will be utilized as the transmit/receive aperture for the final radar demonstration of an NRL base program.

15. SUBJECT TERMS
Cylindrical phased array
Multifunction array

16. SECURITY CLASSIFICATION OF: a. REPORT	b. ABSTRACT	c. THIS PAGE	17. LIMITATION OF ABSTRACT	18. NUMBER OF PAGES	19a. NAME OF RESPONSIBLE PERSON
U	U	U	U	14	Anna Stumme
					19b. TELEPHONE NUMBER *(include area code)* (202) 404-3300

Standard Form 298 (Rev. 8-98)
Prescribed by ANSI Std. Z39.18

This page intentionally left blank.

CONTENTS

This page intentionally left blank.

FIGURES

This page intentionally left blank.

DESIGN OF A CYLINDRICAL ARRAY FOR MULTIFUNCTION USE

1. Introduction

In recent years, the Navy has looked to transition to multifunction array apertures to reduce the size of ”antenna farms” on ships’ masts and other space constrained areas. Cylindrical phased arrays are an attractive aperture for multifunction radio frequency (RF) systems requiring a 360° field of view because of their immense flexibility in radiation pattern performance. Cylindrical arrays offer the pattern versatility to operate with multiple pattern shapes. In one mode, cylindrical arrays form directional patterns that are scanned throughout the azimuth plane with nearly constant gain, beamwidth, sidelobe level (SLL), and polarization properties – avoiding the degradation faced by multi-faced planar array systems [1][2]. In another mode, omni-directional patterns are easily formed with the possibility of adaptive nulling to reduce interference [3]. These advantages have led to their use for radar applications [4] including weather radar [5] and monopulse applications [6], functions including custom pattern shaping including tactical air navigation (TACAN) [7], and are even seen as a technology enabler for millimeter wave (mmW) mobile communications [8][9].

Apertures must support a wide operational bandwidth to support wide-ranging functions. The literature on wideband cylindrical arrays is limited as the half-wavelength circumferential spacing needed to mitigate the impact of distortion modes, combined with the wedge shape of the unit cell, makes integrating wideband elements - which are often long in length - a design and integration challenge. Printed circuit board (PCB) realizations include wideband planar patch elements [10] and long slot elements [11].

Cylindrical arrays, however, are not as widely used as their utility would suggest. This is partially due to increased difficulty in their design and manufacturing that results from the more complex geometry compared to the more well known linear and planar arrays. Techniques, including 3D printing, have been used for simplified manufacturing of circular arrays [12], but all metal designs are preferred for other applications because of their power-handling capabilities, smoother surface finish, and greater mechanical strength [13]. This report presents the design of an all-metal cylindrical array of stepped-notch elements, which will be utilized as the transmit/recieve aperture for the final radar demonstration for a base program (WU 6B10).

2. Cylindrical Array Design

The array design presented in Fig. 1(a) is a cylindrical array with an outer diameter of 12in. The array is comprised of step notch antenna elements, as seen in Fig. 1(c), arranged in 8 element columns, shown in Fig. 1(b), with 64 columns arranged to form a cylinder. By stacking multiple elements in elevation to form column elements, wide-angle scanning can be performed in elevation. Inter-element spacing in both azimuth and elevation (circumferentially and vertically) was set to $\lambda/2$ at the high frequency, 10 GHz, to obtain critical sampling.

Manuscript approved September 29, 2021.

The step notch elements were designed and optimized to operate over 2-10 GHz. This design process is outlined in detail in [14], which starts by decomposing the full array simulation down to a single unit cell simulation with the appropriate boundary conditions. This is done to avoid computationally taxing and long simulation times experienced through full array simulation. The unit cell simulation setup, as proposed in [15] and further extended in [14], for the cylindrical array design is seen in Fig. 2. Periodic boundaries on the non-parallel sides of the unit cell are applied with a $m\frac{2\pi}{N}$ phase shift, simulating all phase modes $m = 0, 1, ..., N-1$. This process results in full characterization of the active reflection coefficents and scattering matrix of the array, as well as the embedded element patterns through post processing computation of the unit cell simulation results.

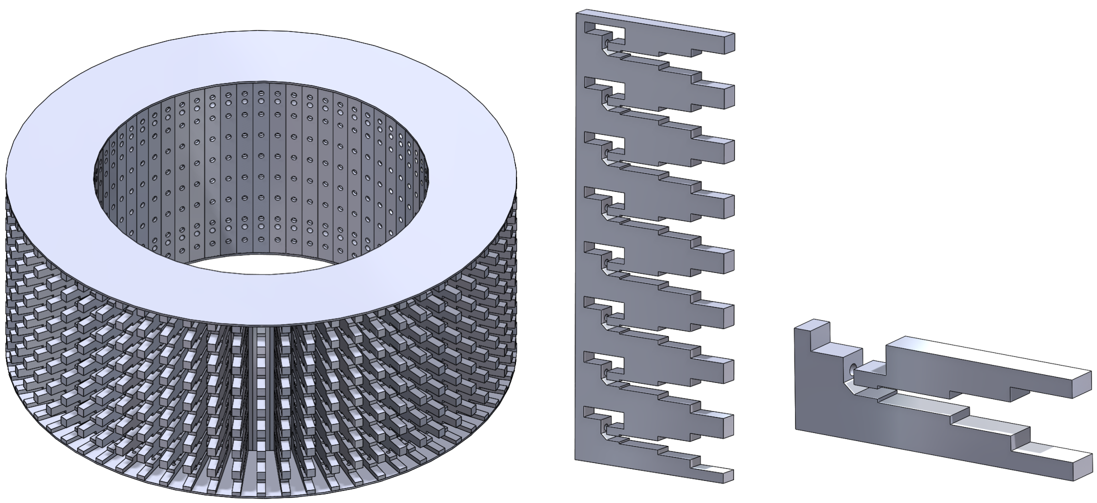

(a) Array design (b) Column element (c) Step notch element

Fig. 1 — Cylindrical array design.

The step notch element was designed and simulated to be well matched over the desired 2-10 GHz operational bandwidth. This was achieved, as seen in Fig. 3, with $\Gamma \leq -10dB$, across the entire frequency band, in otherwords a VSWR of at least 2:1.

From the simulation method described in Section 2, the embedded element patterns and active reflection coefficient data were obtained. In Fig. 4(a), the active reflection coefficient vs. frequency and phase mode is shown. The well matched, or useable modes, are well defined by the theoretical limits as defined in (1). Keeping the phase mode index m as $|m| < m_{max}$ ensures only well matched modes are used.

$$m_{max} = \pm\frac{2\pi}{\lambda}R \tag{1}$$

This theoretical limit is shown in Fig. 4(a) with the solid white lines, showing good agreement between the theoretical limit and simulated results. It is seen that as the frequency increases, the number of useable

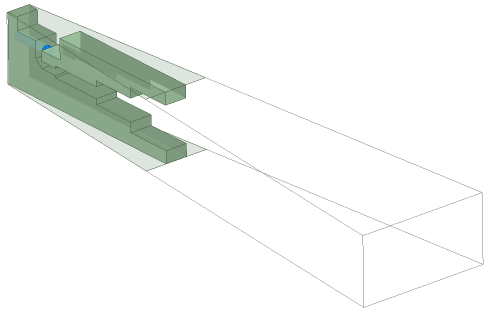

Fig. 2 — HFSS unit cell simulation setup

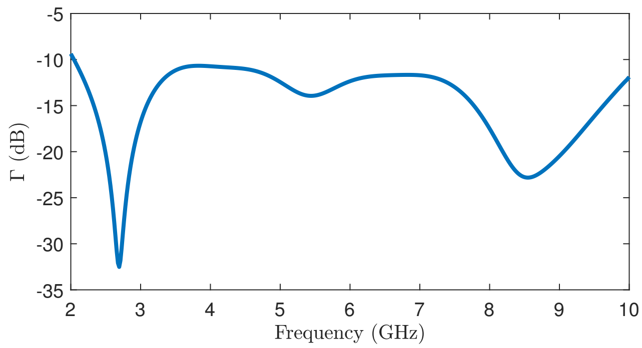

Fig. 3 — Element match

modes also increases. This is seen more clearly in Fig. 4(b), where the active reflection coefficient vs. phase mode index is shown for select frequencies. The modes are well matched ($\Gamma < -10dB$) according to (1), with the useable modes, $|m| < m_{max}$, well matched, and modes $|m| > m_{max}$ exibiting near perfect reflection.

Embedded element, Fig. 5(a), and column patterns, Fig. 5(b), are shown in Fig. 5 at select frequencies within the 2-10 GHz operating band. These are used for comparison with the measured results presented in Section 3. Embedded element patterns are obtained by exciting a single element within a column element, whereas a column pattern is obtained by exciting all 8 elements within a column uniformly.

3. Array Fabrication and Results

The cylindrical array design, shown in Fig. 7(a), was fabricated using electrical discharge machining, or EDM. Due to the rotational relationship between the column elements, the array elements cannot be machined in one piece. Instead, the individual column elments are machined seperately using EDM, as seen in Fig. 6. Additionally, the top and bottom panels and the inner ground plane are machined. The ground plane is machined in sections for easier assembly. All parts have appropriate screw or clearance holes to accomodate assembly and to electrically ground the entire array structure together, as shown in Fig. 7(a). The final assembled array is seen in Fig. 7(b), in the anechoic measurement chamber.

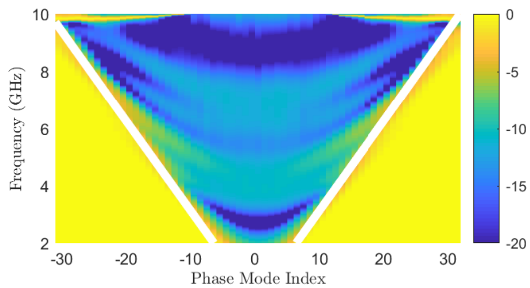

(a) Active reflection coefficient contour plot

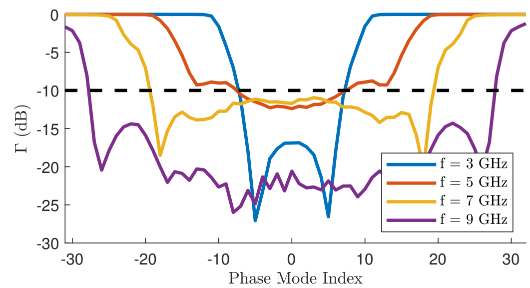

(b) Active reflection coefficient at select frequencies

Fig. 4 — Active reflection coefficient, Γ.

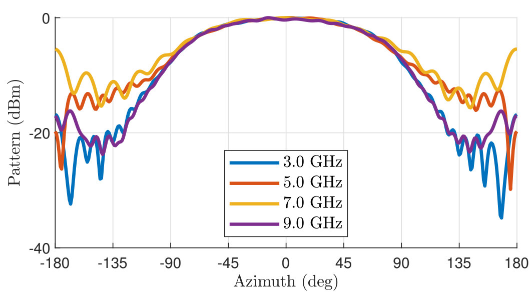

(a) Simulated embedded element patterns

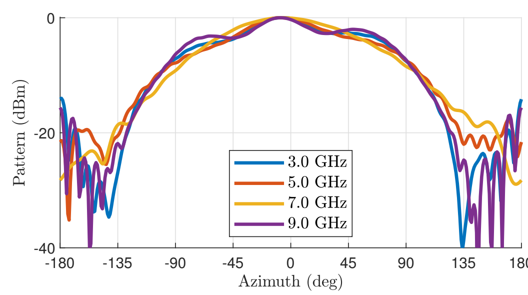

(b) Simulated column patterns

Fig. 5 — Simulated patterns at select frequencies.

Once fabricated, the array seen in Fig. 7(b) was characterized in an anechoic chamber through a series of measurements. Embedded element patterns, column patterns, and gain measurements were taken and compared to simulated data. Embedded element patterns were measured for a center element in the array. Measured embedded element patterns across select frequencies in the band are shown in Fig. 8(a) with comparisons to the simulated patterns shown in Fig. 9. Column patterns were measured using an 8-way power divider feeding each element in a single column with uniform amplitude. Gain was measured for the embedded element pattern across the bandwidth as shown in Fig. 11.

4. Beamforming for Radar Demonstration

As mentioned in Section 1, the cylindrical array presented will be utilized in a radar demonstration for the base program WU 6B10. The radar demonstration will be conducted at X-band utilizing 8 column elements of the array. Using only 8 elements the angular sector of the array covers 45 deg, instead of the full 360 deg if all 64 column elements were utilized. As such, the radar demo will show scanning over a 30 deg sector in 5 deg increments.

Fig. 6 — Fabricated column element using EDM

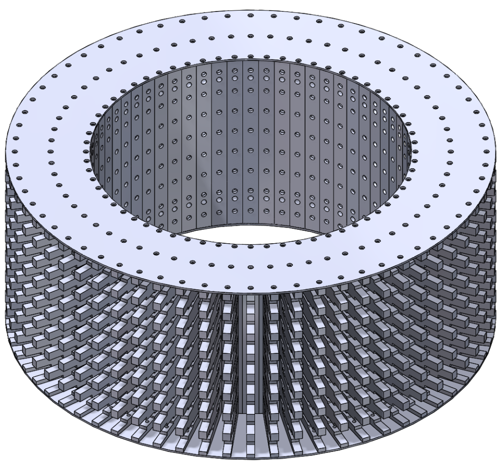

(a) Array design

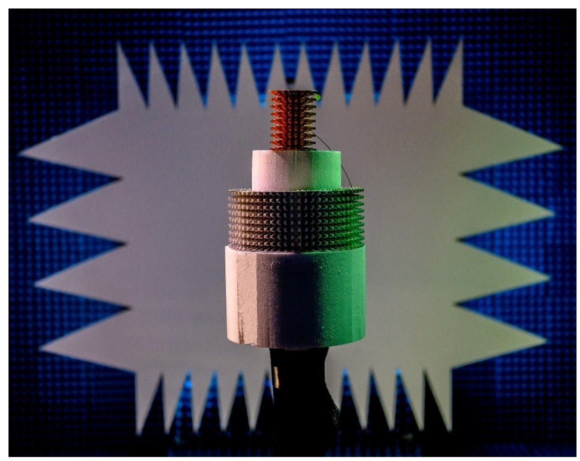

(b) Array fabricated

Fig. 7 — Final array design including assembly screw holes. (a) Array design with appropriate screw holes for assembly. (b) The array in the middle of the picture, or larger array on the bottom, is the fabricated and assembled array. Array is set up in the anechoic chamber for measurements.

To perform directonal beam scanning with a cylindrical array the weighting technique from [4] is used, where phase-only weights are computed using (2).

$$w_n = \frac{\beta}{|[\mathbf{f}_{mb}]_n|}[\mathbf{f}_{mb}]_n \tag{2}$$

From measuring each of the 8 column elements to be used in the demo, we obtain the column patterns seen in Fig. 12(a). Each pattern points in a unique direction due to the unique pointing angle of the elements

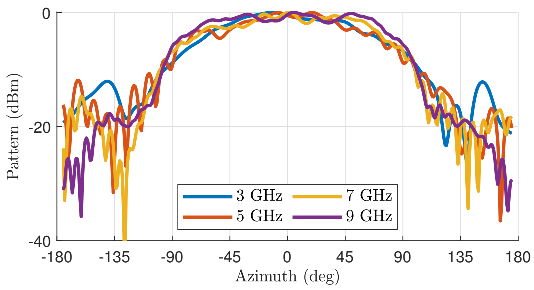

(a) Embedded element patterns

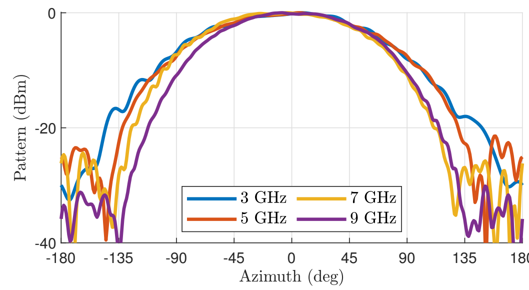

(b) Column patterns

Fig. 8 — Measured patterns for select frequencies across the bandwidth. (a) Embedded element patterns for a center element in a column. (b) Column pattern.

caused by the rotational realtionship between elements. By applying the weights calculated using (2) for each scan angle of ± 15, using 5 deg increment,s results in the directional patterns seen in Fig. 12(b).

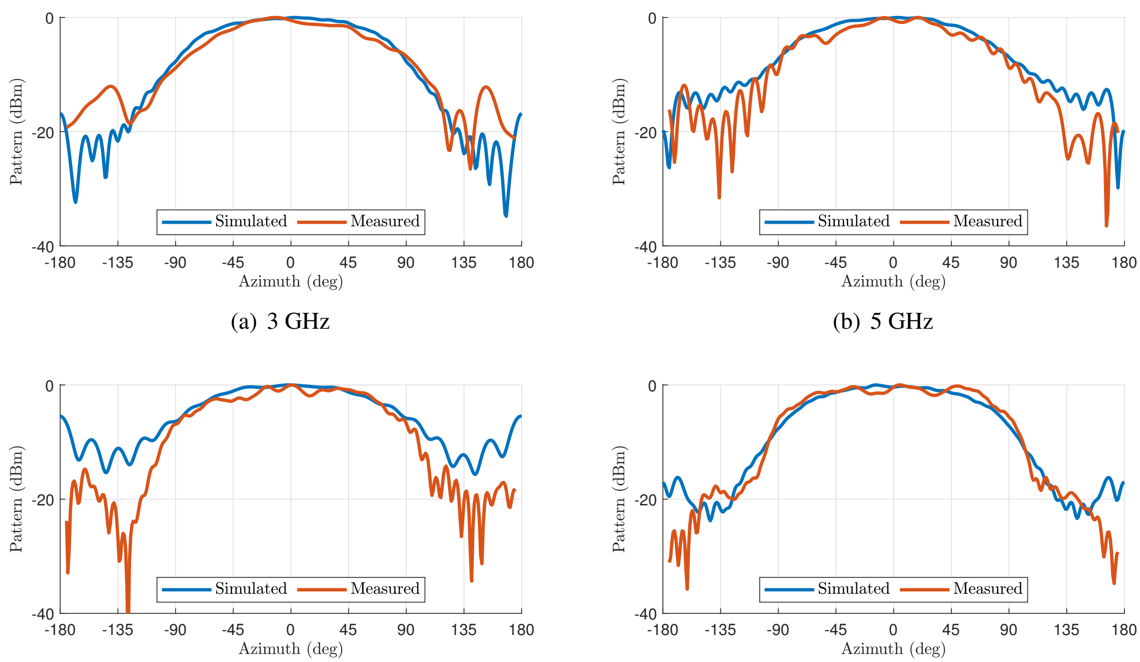

(a) 3 GHz (b) 5 GHz

(c) 7 GHz (d) 9 GHz

Fig. 9 — Comparison between simulated and measured embedded element patterns for select frequencies.

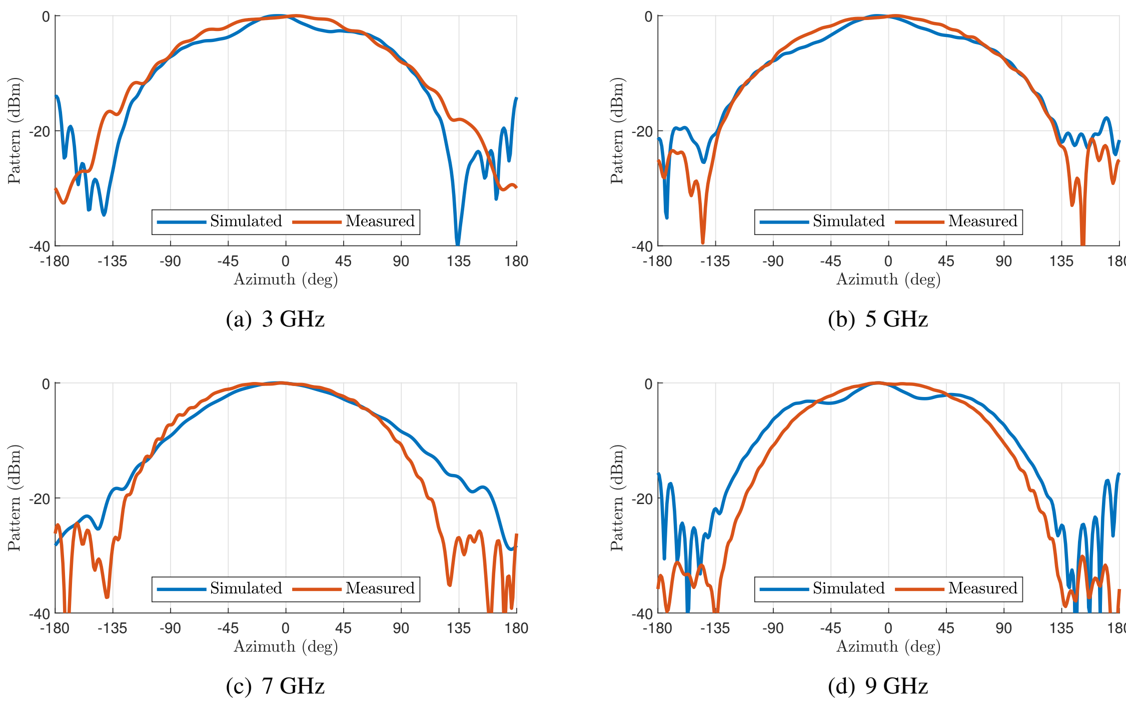

(a) 3 GHz (b) 5 GHz (c) 7 GHz (d) 9 GHz

Fig. 10 — Comparison between simulated and measured column patterns for select frequencies.

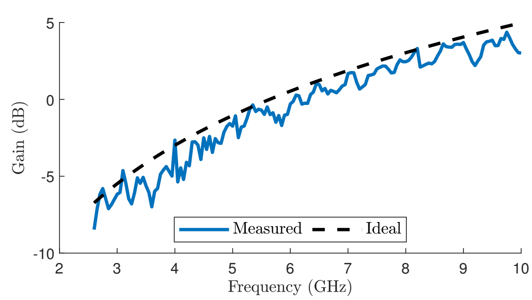

Fig. 11 — Gain of element with respect to the ideal gain.

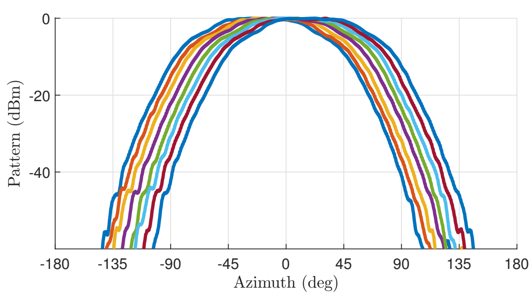

(a) 8 column patterns

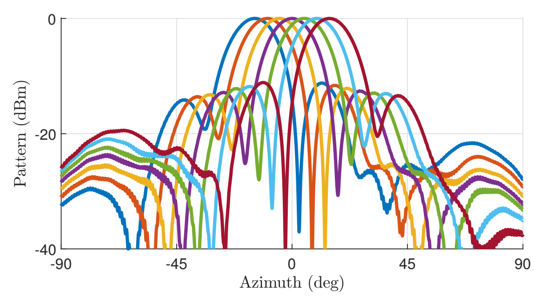

(b) Scanned directional patterns

Fig. 12 — **(a)** Measured column patterns for the 8 column elements to be used in the demo. The shift in pointing direction between the patterns correlates to the angular distance between each element. **(b)** Scanned directional patterns over the ± 15 deg scan area desired.

5. Conclusions

This report presents the design, fabrication, and measurements of an all-metal cylindrical array of stepped-notch elements. This array will be the transmit/recieve aperture for the final radar demonstration for a base program (WU 6B10) using phase-only weights to form directional beams over a small scan area. Simulated and measured results show good agreement for both embedded element and column patterns indicating successful design and fabrication of the array. Measured column patterns and computed, scanned directional patterns demonstrate sucessful beam steering capabilities over a small sector. Success with directional beam steering over a small sector with 8 elements indicates that using all 64 column elements should enable full 360deg scanning capabilities.

REFERENCES

[1]G. Galati, F. Madia, P. Carta, E. G. Piracci, R. Stallone, and M. Massardo, “Time for a change in phased array radar architectures - part i: Planar vs. conformal arrays,” in *2015 16th International Radar Symposium (IRS)*, 2015, pp. 912–917.

[2]G. Galati, F. Madia, P. Carta, E. G. Piracci, S. Franco, and S. Quattrociocchi, “Time for a change in phased array radar architectures- part ii: The d-radar,” in *2015 16th International Radar Symposium (IRS)*, 2015, pp. 918–923.

[3]R. Mital and W. M. Dorsey, “Fast synthesis of multiple nulls in an omnidirectional pattern,” in *2017 IEEE International Symposium on Antennas and Propagation USNC/URSI National Radio Science Meeting*, 2017, pp. 2011–2012.

[4]W. M. Dorsey and D. P. Scholnik, “Transmit and receive circular array pattern synthesis for radar applications,” in *2016 IEEE Radar Conference (RadarConf)*, 2016, pp. 1–6.

[5]G. Zhang, R. Palmer, L. Lei, R. J. Doviak, D. S. Zrnic, and Y. Al-Rashid, “Polarimetric phased array radar for weather measurement: Issues and solutions,” in *2011 IEEE RadarCon (RADAR)*, 2011, pp. 590–591.

[6]W. M. Dorsey and J. O. Coleman, “Socp design of monopulse sum and difference beams for a uniform circular array,” in *2017 IEEE 18th Wireless and Microwave Technology Conference (WAMICON)*, 2017, pp. 1–4.

[7]W. M. Dorsey, J. O. Coleman, and W. R. Pickles, “Transmit TACAN bearing information with a circular array,” *Hindawi International Journal of Antennas and Propagation*, vol. 2015, no. 846720.

[8]T. S. Rappaport, S. Sun, R. Mayzus, H. Zhao, Y. Azar, K. Wang, G. N. Wong, J. K. Schulz, M. Samimi, and F. Gutierrez, “Millimeter wave mobile communications for 5G cellular: It will work!” *IEEE Access*, vol. 1, pp. 335–349, 2013.

[9]J. Zhang, X. Ge, Q. Li, M. Guizani, and Y. Zhang, “5g millimeter-wave antenna array: Design and challenges,” *IEEE Wireless Communications*, vol. 24, no. 2, 2017.

[10]M. Abbaspour and H. R. Hassani, “Wideband planar patch antenna array on cylindrical surface,” *IEEE Antennas and Wireless Propagation Letters*, vol. 8, pp. 394–397, 2009.

[11]J. Rayno, N. Celik, and M. F. Iskander, “Dual-polarization cylindrical long-slot array (clsa) antenna integrated with compact broadband baluns and slot impedance transformers,” *IEEE Antennas and Wireless Propagation Letters*, vol. 12, pp. 1384–1387, 2013.

[12]W. M. Dorsey, A. Stumme, K. M. Charipar, and N. A. Charipar, “3-d-printed circular array for wimax base station,” *IEEE Antennas and Wireless Propagation Letters*, vol. 18, no. 6, pp. 1159–1163, 2019.

[13]R. Kindt and R. Pickles, “12-to-1 bandwidth all-metal vivaldi array element,” in *2009 IEEE Antennas and Propagation Society International Symposium*, 2009, pp. 1–4.

[14]W. Dorsey, A. Stumme, and J. Coleman, “Tutorial: Applying phase-mode theory to the design of cylindrical arrays,” Naval Research Laboratory, Washington, DC, Tech. Rep. NRL/MR/5310–19-9915, August 2019.

[15] C. J. Fulton and A. Mirkamali, "A computer-aided technique for the analysis of embedded element patterns of cylindrical arrays [em programmer's notebook]," *IEEE Antennas and Propagation Magazine*, vol. 57, no. 3, pp. 132–138, June 2015.